Coupling between electronic and structural degrees of freedom in the triangular lattice conductor Na_xCoO_2

Q. Huang,[1] M. L. Foo,[2] R. A. Pascal, Jr.,[2] J. W. Lynn,[1] B. H. Toby,[1] Tao He,[3] H. W. Zandbergen,[4] and R. J. Cava[2]
[1]*NIST Center for Neutron Research, National Institute of Standards and Technology, Gaithersburg, Maryland 20899, USA*
[2]*Department of Chemistry, Princeton University, Princeton, New Jersey 08540, USA*
[3]*DuPont Central Research and Development Experimental Station, Wilmington, Delaware 19880, USA*
[4]*National Centre for HREM, Department of Nanoscience, Delft Institute of Technology, Al Delft, The Netherlands*
(Received 3 June 2004)

The ambient temperature crystal structures of compounds in the Na_xCoO_2 family, for $0.34 < x \leqslant 1.0$, determination by powder neutron diffraction, are reported. The structures consist of triangular CoO_2 layers with Na ions distributed in intervening charge reservoir layers. The shapes of the CoO_6 octahedra that make up the CoO_2 layers are found to be critically dependent on the electron count and on the distribution of the Na ions in the intervening layers, where two types of Na sites are available. Correlation of the shapes of cobalt-oxygen octahedra, the Na ion positions, and the electronic phase diagram in Na_xCoO_2 is made, providing an example of how structural and electronic degrees of freedom can be coupled in electrically conducting triangular lattice systems.

DOI: XXXX PACS number(s): 61.66.Fn, 61.12.Ld, 61.50.Nw

INTRODUCTION

Square planes of metals and oxygen form the basis for scientifically and technologically important materials such as perovskite ferroelectrics, superconductors, and ferromagnets. Triangular arrangements of metals and oxygen are much less generally studied, except in the context of magnetism in electrically insulating materials, where the placement of antiferromagnetically coupled magnetic atoms in triangle-based lattices leads to frustration of the low-temperature magnetic state.[1] The introduction of charge carriers into such triangular magnetic lattices in sufficient number to yield metallic conductivity has been a goal of research for some time. Na_xCoO_2, with a crystal structure consisting of alternating layers of Na ions and triangular CoO_2 layers, is the embodiment of such a system. (The CoO_2 layers consist of a sandwich of triangular O, Co, and O planes.) The charge on the CoO_2 layers is controlled by the degree of filling of the Na layer—in a manner fully analogous to the relationship between the charge reservoir layers and the CuO_2 planes in the high-T_c superconductors.[2] The properties of Na_xCoO_2 are not disappointing: a high thermoelectric power metallic conductor is found for $Na_{0.7}CoO_2$,[3,4] superconductivity is induced in $Na_{0.35}CoO_2$ when it is intercalated with water,[5] and $Na_{0.5}CoO_2$ appears to be insulating at low temperatures due to ordering of Co ion charges.[6] Compounds based on square-based transition-metal–oxygen lattices display a broad range of effects due to the coupling of electronic, magnetic, and structural degrees of freedom, but until now there has been no model system for investigating such effects in triangle-based electronic conductors. Here we report structural studies of the average crystal structure of Na_xCoO_2 over a wide range of Na content in the charge reservoir layer. Changes in the electron count due to changing Na content strongly affect the structure of the CoO_2 plane. The results suggest that conducting triangular lattice systems display their own class of structural and electronic coupling phenomena distinct from those previously studied in square-based systems.

Hexagonal Na_xCoO_2, which has two triangular CoO_2 layers per unit cell, has been reported to exist for $0.25 < x < \sim 0.8$.[6–13] It exhibits metallic behavior for a wide range of x, with the exception of $x = 1/2$, where an insulating state is found at low temperatures.[6] Magnetic ordering has been reported for compositions near $Na_{0.75}CoO_2$.[7–9] Na contents lower than 0.7 in Na_xCoO_2 can only be obtained by room temperature deintercalation of sodium from $Na_{0.7}CoO_2$, and in one case crystals grown by the floating zone technique have been reported to have $x > 0.75$.[9] Crystal structures have been reported for some Na_xCoO_2 compositions,[10–13] and $Na_{0.3}CoO_2$ has recently been studied by neutron diffraction due to its importance as the host for the superconducting phase.[14,15] An electron diffraction study of the Na_xCoO_2 series[16] has revealed a complex series of ordered Na distributions at different Na compositions.

This report describes the results of crystal structure determinations by powder neutron diffraction of a series of samples with x between 0.34 and 1.0 in Na_xCoO_2, with an eye toward interpreting the electronic phase diagram. Because the Na charge is donated to the CoO_2 layers, this represents a change in the formal oxidation state of Co from $Co^{3.66+}$ to Co^{3+}. Although the basic two-layer hexagonal structure is maintained over the whole compositional range, we find substantial changes in the Na ion distribution as a function of composition, accompanied by significant changes in the geometry of the CoO_2 layer due to the changing electron count. The results indicate the presence of strong coupling between structural and electronic degrees of freedom in this system.

EXPERIMENT

$Na_{0.75}CoO_2$ was made by solid-state synthesis. Na_2CO_3 and Co_3O_4 in amounts corresponding to $Na_{0.77}CoO_2$ were mixed and heated to 800 °C under flowing O_2 for 16 h. Due

to the volatility of Na oxides, the final Na composition is slightly lower than the starting composition. A sample of $Na_{0.34}CoO_2$ was prepared by stirring 1 g of $Na_{0.75}CoO_2$ with 1× of NO_2PF_6 in dry acetonitrile under argon for 2 days ("1×" indicates that the amount of NO_2PF_6 used is exactly the amount that would theoretically be needed to remove all the sodium from $Na_{0.7}CoO_2$). It is noted that this method produced $NaNO_3$ as a by-product. To prepare $Na_{0.5}CoO_2$, $Na_{0.75}CoO_2$ (1 g) was stirred in 120 ml of a 10× solution of I_2 in acetonitrile for 4 days. $Na_{0.64}CoO_2$ was prepared by stirring $Na_{0.75}CoO_2$ (1 g) in 40 ml of a 0.5× solution of I_2 in acetonitrile for 4 days. The products in all cases were washed with dry acetonitrile, dried in argon, and stored an argon-filled glovebox.

For the synthesis of samples for $x > 0.75$, sodium metal (0.3 g) and tetrahydrofuran (40 ml) were placed in a 25 mm × 150 mm Pyrex screw-capped tube, and were heated by placing the lower 25 mm in an oil bath maintained at 95 °C. After 1 h, benzophenone (2.0 g) was added. After heating another hour, powdered $Na_{0.75}CoO_2$ (1.5 g) was added, and the mixture was heated, with agitation by a magnetic stirring bar, for 48 h. The mixture was cooled to room temperature, and ethanol (20 ml) was added to destroy the benzophenone ketyl radical anion and any unreacted sodium metal. After 20 min, the mixture was centrifuged for 3 min at 2000 g in a stainless-steel centrifuge tube. The organic supernatant was decanted, the solid was resuspended in dichloromethane (20 ml), the mixture was centrifuged, and the organic supernatant was again decanted. Two more dichloromethane washes were performed in the same manner, and then the final black pellet was broken up and air dried overnight to yield 1.3 g of sodium-enriched material. This process led in two different syntheses to materials of overall stoichiometry $Na_{0.82}CoO_2$ and $Na_{0.89}CoO_2$. As described below, this difference may be due to the presence of a two-phase region in the phase diagram at these compositions, or possibly due to uncertainties in the temperature of the reaction. The sodium contents of the samples were determined by multiple independent composition measurements by the ICP-AES method, and are considered to be reliable to ±0.02/formula unit. For all samples the Na content of the constituent phases was unambiguously determined through the structural refinements.

The neutron powder diffraction intensity data for the Na_xCoO_2 samples were collected using the BT-1 high-resolution powder diffractometer at the NIST Center for Neutron Research, employing a Cu (311) monochromator to

TABLE I. Structure parameters of Na_xCoO_2 at room temperature. Space group $P6_3/mmc$. Atomic positions: Co, 2*a* (0,0,0); Na(1), 2*b* (0,0,1/4) the structure types *H*1 and *H*2; Na(2), 6*h* (2*x*,*x*,1/4) for structure type *H*1 or 2*c* (2/3,1/3,1/4) for structure types *H*2 and *H*3; O, 4*f* (1/3,2/3,*z*).

x (chem.)	nd[a]	[0.49][b]	0.64	0.75		nd	0.89	
x (refined)	0.34	[0.56]	0.63	0.71	0.77	0.76	0.80	1
Structure type	*H*1	*O*1	*H*1	*H*1 (31.1%)	*H*2 (68.9%)	*H*2	*H*2 (56.9%)	*H*3 (43.1%)
a (Å)	2.8129(1)	[2.81508(3)]	2.82438(6)	2.8314(9)	2.84126(6)	2.84182(4)	2.8555(1)	2.8829(1)
c (Å)	11.2152(6)	[11.1296(2)]	11.0046(3)	10.8756(4)	10.8144(3)	10.8070(3)	10.7024(6)	10.4927(6)
V (Å^3)	76.848(8)	[76.382(2)]	76.024(4)	75.867(5)	75.606(4)	75.583(2)	75.576(9)	75.524(9)
Co *B* (Å^2)	0.15(7)	[0.49(4)]	0.26(4)	0.36(3)	0.36(3)	0.33(7)	0.21(6)	0.21(6)
Na(1) *B* (Å^2)	1.0	[2.9(2)]	1.7(2)	1.3(1)	1.3(1)	1.3(2)	1.19(7)	1.19(7)
n	0.12(1)	[0.264(9)]	0.220(9)	0.194(19)	0.226(10)	0.221(12)	0.112(12)	0
Na(2) *x*	0.292(4)		0.289(2)	0.271(3)				
B (Å^2)	1.0	[2.9(2)]	1.7(2)	1.3(1)	1.3(1)	1.3(2)	1.19(7)	1.19(7)
n	0.074(4)	[0.294(8)]	0.137(7)	0.171(9)	0.543(13)	0.544(16)	0.688(14)	1
O *z*	0.0855(2)	[0.08744(8)]	0.0887(1)	0.0904(2)	0.0909(1)	0.0907(2)	0.0936(2)	0.0936(2)
B (Å^2)	0.80(3)	[0.66(2)]	0.59(2)	0.54(2)	0.54(2)	0.58(3)	0.59(2)	0.59(2)
R_p (%)	4.25	[4.34]	4.82	6.24		2.77	5.10	
R^{wp} (%)	5.26	[5.83]	5.74	5.10		3.33	6.46	
χ^2	1.244	[2.855]	0.9538	0.9404		1.015	1.501	
Selected bond (å) distances and angles (degrees)								
Co—O ×6	1.886(1)	[1.8944(5)]	1.9004(5)	1.911(1)	1.9125(7)	1.911(1)	1.932(1)	1.929(1)
Na(1)—O ×6	2.458(2)	[2.4321(7)]	2.4104(8)	2.387(2)	2.3770(9)	2.378(2)	2.378(2)	
Na(2)—O ×4	2.400(2)	[2.4321(7)]	2.345(3)	2.300(4)	2.3770(9)	2.378(2)	2.338(2)	2.349(1)
×2	2.60(1)	[2.4321(7)]	2.566(8)	2.61(1)	2.3770(9)	2.378(2)	2.338(2)	2.349(1)
O—Co—O	83.57(7)	[84.02(3)]	84.01(4)	84.05(8)	84.10(4)	83.94(8)	83.52(8)	83.52(7)

[a]This sample contains 23% $NaNO_3$; it was taken into account in the refinement.

[b]Orthorhombic structure. Refinement in hexagonal symmetry for comparison purposes only. Reference 18 reports orthorhombic refinement.

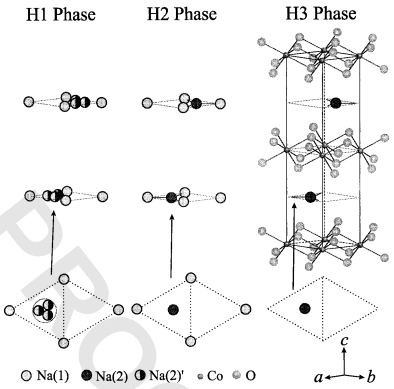

FIG. 1. The three hexagonal structure types found for Na_xCoO_2. Layers of edge-shared CoO_6 octahedra are seen in a triangular lattice with Na ions occupying ordered or disordered positions in the interleaving planes. Three different Na ion sites are found. In the $H1$ phase, $0.3<x0.75$, (with the exception of $x=0.5$) Na atoms partially occupy the Na(1) $2b$ and Na(2)′ $6h$ sites. In the $H2$ phase, $0.76<x<\sim 0.82$, the Na(1) and Na(2) $2c$ sites are occupied. In the $H3$ phase, $x=1$, only the $2c$ site sites are occupied.

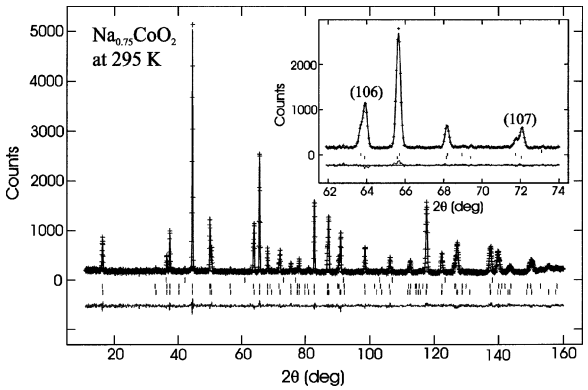

FIG. 2. Observed (crosses) and calculated (solid line) intensities for $Na_{0.75}CoO_2$. Vertical lines indicate the Bragg peak positions for the phases $H2$ (bottom), $H1$ (middle), and 0.4 wt % CoO impurity (top). Differences between the observed and calculated intensities are shown in the bottom of the figure. The inset shows a portion of the pattern illustrating that the (106) and (107) reflections are good indications of the different lattice parameters for the phases $H2$ and $H3$ in this sample with overall composition $Na_{0.75}CoO_2$.

produce a neutron beam of wavelength 1.5403 Å. Collimators with horizontal divergences of 15′, 20′, and 7′ of arc were used before and after the monochromator, and after the sample, respectively. The intensities were measured in steps of 0.05° in the 2θ range 3°–168°. The structural parameters were refined using the program GSAS.[17] The neutron scattering amplitudes used in the refinements were 0.363, 0.253, and 0.581 ($\times 10^{-12}$ cm) for Na, Co, and O, respectively.

RESULTS

The structural refinements were carried out in the space group $P6_3/mmc$. The Co and O positions, and one of the possible Na positions [Na(1), in site $2b$ $(0,0,1/4)$] were found to be unambiguously defined for all compositions. Taking the $x=0.64$ sample as an example, we found that the Na(2) atom, in the site $2c$ $(2/3,1/3,1/4)$, displayed a large temperature factor, ~ 3.0 Å^2, when the diffraction data were fitted with one of the models previously reported for $Na_{0.3}CoO_2$.[14] A refinement with Na(2) at the $6h$ $(2x,x,1/4)$ site [labeled as the Na(2)′ site], a model previously reported[15] for $x=0.61$, allows for displacements of the Na(2) atoms from the centers of the ideal triangular prismatic coordination polyhedra at $(2/3,1/3,1/4)$. This model gave a substantially better agreement index and a more reasonable temperature factor for this Na. The possibility of a displaced position for Na(2) was therefore considered in the analysis for all compositions: if the x coordinate for the Na(2)′ ions at the $6h$ $(2x,x,1/4)$ site converged to $x=1/3$, then the Na was considered to be in the Na(2) $2c$ $(2/3,1/3,1/4)$ site. Satisfactory refinements were obtained for all compositions within these models.

The crystal structures of the three phases found in the Na_xCoO_2 series (Table I) are shown schematically in Fig. 1. The compounds over the composition range from $0.34<x<0.74$ (with the exception of $x=0.5$) are well described by a structure in which the Na(1) site is partially occupied and the Na(2) ions are displaced from the ideal centers of the NaO_6 triangular prisms, i.e., in the Na(2)′ sites. This structure type[15] covers a large fraction of the phase diagram, and is designated as the $H1$ phase. Separated by a narrow two-phase region from the $H1$ phase, a different structure type is found for $0.76<x<\sim 0.82$. This phase, designated as $H2$, has all the Na(2) ions directly in the center of the ideal Na(2) triangular prism, as well as Na ions in the Na(1) site. The sample of overall Na stoichiometry $Na_{0.75}CoO_2$ is a mixture of the $H1$ and $H2$ phases and clearly shows the presence of the two-phase region (Fig. 2). It is of interest that the change in position from Na(2)′ to Na(2) sites is abrupt, indicating that at a critical Na layer filling the system suddenly favors on-center Na(2) ion occupancy. The reason for this behavior is not yet understood.

Finally, a distinct phase [designated $H3$] is found at composition $NaCoO_2$ after another two-phase region. In this compound, all the Na(1) sites are empty and all the Na(2) sites are filled: the Na are all in ideal trigonal prismatic sites that share only edges with the CoO_6 octahedra. The crystal structure of $H3$ is distinctly different from that of the thermodynamically stable phase $NaCoO_2$, which has all the Na in octahedral coordination with oxygen.[12]

Figure 3 shows some of the structural characteristics of the Na_xCoO_2 phases in more detail. For Na(1), the coordination polyhedron is a regular triangular antiprism. The Na(1) position shares faces with CoO_6 octahedra in the planes directly above and below, a situation that leads to significant Na—Co ion repulsion, suggesting that this position is relatively higher in energy than the Na(2) and Na(2)′ positions. The Na(2) position is at the center of the regular triangular antiprisms that share only edges with the CoO_6 octahedra. When a particular Na(2) or Na(2)′ site is occupied, then its nearest-neighbor Na(1) sites are excluded from occupancy, as they are too close. The Na(2)′ sites are displaced from the centers of the regular antiprisms. We believe that this off-

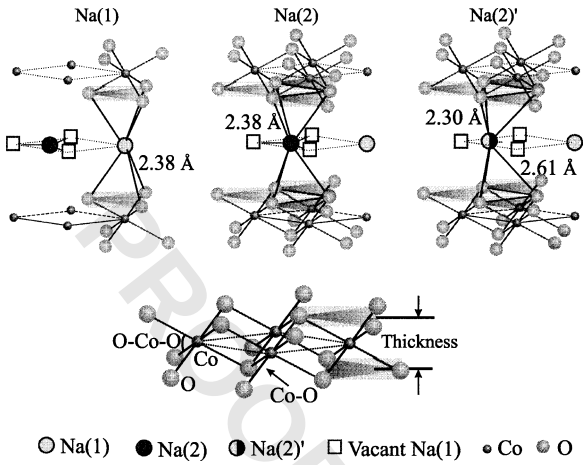

FIG. 3. Selected structural components in Na_xCoO_2. Upper figure: the triangular prismatic NaO_6 coordination polyhedra. The Na(1) ion (2*b* site) triangular prisms share faces with the CoO_6 octahedra. The Na(2) ion (2*c* site) regular triangular prisms share edges with the CoO_6 octahedra. The Na(2)′ ions randomly occupy one of the possible the 6*h* sites distributed around the 2*c* site, displaced from the center of the triangular prisms. If a particular Na(2) or Na(2)′ site is occupied, then the nearest Na(1) position is too close to be simultaneously occupied. Lower figure: detail of the CoO_2 layer.

center position of the Na(2)′ is found due to repulsion of the Na(2)′ ion by Na ions in occupied second-nearest-neighbor Na(1) sites. For the *H*1, *H*2, and *H*3 phases (lower part of Fig. 3), the Co—O bond lengths are all the same within the octahedra and the O—Co—O bond angles deviate from 90°, resulting in a significant flattening of the octahedra along an axis perpendicular to the CoO_2 planes.

Figure 4 summarizes the compositional stability regions and general structural characteristics of the four phases found for Na_xCoO_2. (The *O*1 phase is the orthorhombic insulating phase at $Na_{0.5}CoO_2$.[6,18] Schematic representations of the Na ion positions in the charge reservoir layer are at the top of the figure. The presence and extent of the two-phase regions (±0.02 Na per formula unit) have been determined from samples in which the overall Na content was determined by chemical analysis and two phases were observed in the neutron diffraction patterns. The fractional occupancies of the two types of sodium sites are a strong function of total Na content. The Na(1) site, where the Na ion is subject to repulsive interactions with the Co, is occupied for all compositions at a lower probability than the Na(2)′ sites in the *H*1 phase. In the orthorhombic *O*1 phase (x=0.5), however, these two sites are occupied in equal proportions, an indication of the coupling of the Na positions to the charge distribution in the underlying Co lattice.[6,18] As the Na content increases from x=0.5 towards x=0.75, the added Na fills the Na(2)′ sites only. In the *H*2 phase, the Na(1) site occupancy decreases dramatically with increasing Na concentration, and the Na(2) sites becomes more and more preferentially occupied. A discontinuous change in the occupancies is apparent at $x \approx 0.8$: in the *H*3 phase all the possible Na(2) sites are occupied and the Na(1) sites are all empty.

The crystallographic *a* axis, representative of the in-plane size of the CoO_6 octahedra, increases in a manner consistent

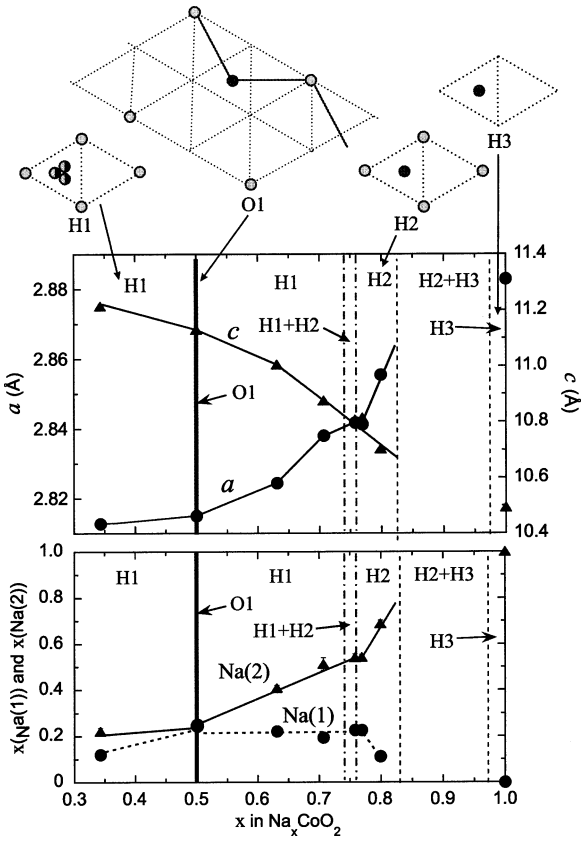

FIG. 4. The general structural characteristics and compositional stability regions of the four Na_xCoO_2 phases, designated as *H*1, *H*2, *H*3, and *O*1. Upper panel, hexagonal crystallographic cell parameters. Lower panel, fractional occupancies of the two types of sodium sites: Na(1) shares faces with the CoO_6 octahedra, and Na(2)′ and Na(2) (plotted as one site) share edges with the CoO_6 octahedra. Above the panels, the sodium ion distributions in the four phases are shown schematically.

with decreasing the formal oxidation state of Co with increasing Na content in Na_xCoO_2. The shrinkage of the *c* axis lattice parameter with increasing Na content is a summation of two different effects. As the fractional occupancy of Na in the charge reservoir layer increases, the increasing positive charge results in an increasing Coulombic attraction between neighboring CoO_2 layers, and their separation decreases. This is shown in the upper panel of Fig. 5, which plots the thickness of a single NaO_2 layer (the CoO_2—CoO_2 layer separation) as a function of Na content. This CoO_2—CoO_2 layer separation changes continuously in the *H*1 phase, but there is a pronounced decrease in the *H*2 phase, in the composition region where all the Na(1) sites are being depopulated. This suggests that the Na(1) ion repulsion with the Co in CoO_6 octahedra directly above and below that share faces with it contributes significantly to pushing the layers apart. The overall trend to decreasing NaO_2 layer thickness is continued on passing from the *H*2 to the *H*3 phase.

The thickness of a single CoO_2 layer (Fig. 5) varies in a complex manner with composition, and indicates that substantial structural changes are taking place as a response to changing electron count in Na_xCoO_2. In the *H*1 phase, the CoO_2 layer thickness increases systematically with increas-

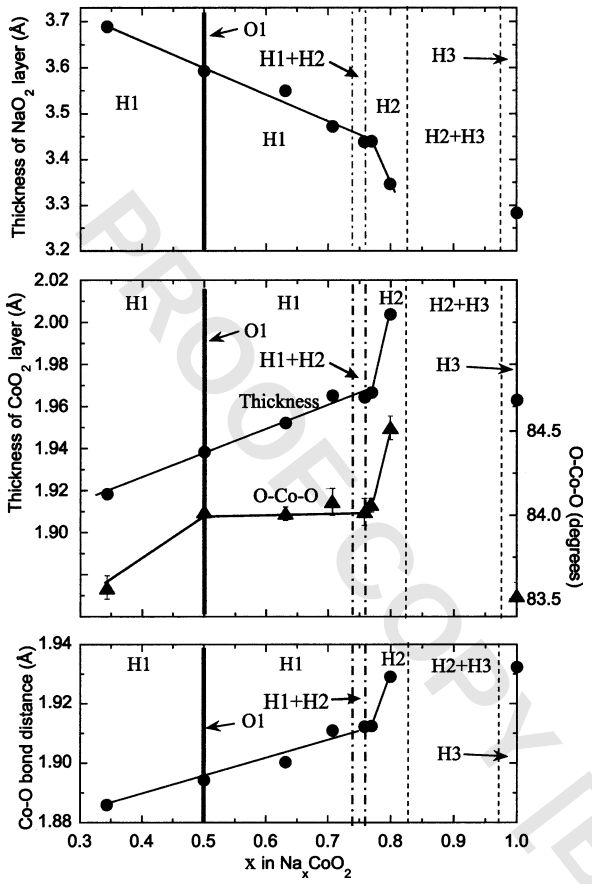

FIG. 5. Upper panel, thickness of the NaO_2 layers (also the separation of the CoO_2 planes) in Na_xCoO_2 as a function of Na content. Middle panel: thickness of the CoO_2 layer and variation in O—Co—O bond angle as a function of Na content. Lower panel: the corresponding variation in Co—O bond length.

ing x, mirroring, as expected, the increasing size of the Co ion. There is a sudden increase in the CoO_2 layer thickness in the $H2$ phase, and, for $NaCoO_2$, the thickness of the CoO_2 layer decreases abruptly. The Co—O bond lengths increase systematically, and as expected, with decreasing formal Co oxidation state in the $H1$ and $O1$ phases. The bond angles, however, first change in the $H1$ phase at low x, and then remain constant for the range of compositions $0.5<x<0.75$. This indicates that the CoO_6 octahedra do not change shape in this electron count region, but rather uniformly expand. In the $H2$ phase there are substantial changes: both the Co—O bond lengths and the O—Co—O bond angles increase. Both of these effects lead to the observed increase of the thickness of the CoO_2 layer in the $H2$ phase within a narrow composition region. Finally, comparison of the Co—O bond lengths in the $H2$ and $H3$ phases at $x=0.8$ and $x=1.0$ indicates that the differences are very small, though the electron count of the CoO_2 layer has changed substantially. Surprisingly, the donation of the 0.2 electrons to the CoO_2 layer on passing from $H2$ to $H3$ is accommodated primarily in a change in the O—Co—O bond angle, not the Co—O bond length.

DISCUSSION

We postulate that the CoO_2 layer thickness is the structural characteristic that most sensitively reflects the electronic state of Na_xCoO_2. For CoO_6 octahedra of ideal shape, the t_{2g} states are energetically degenerate. For octahedra compressed by shortening the distance between opposing triangular faces, as is found in Na_xCoO_2, the degeneracy is partially lifted, yielding two lower energy two-electron t_{2g} suborbitals and one higher energy two-electron t_{2g} suborbital. The greater the compression of the octahedra, the more different in energy the upper and lower t_{2g} suborbitals will be. The relative thickness of the CoO_2 layer is a measure of that compression. Oxides based on Co^{3+} are well known for displaying a delicate balance between different orbital occupancies, and different spin states, based on both structural distortion and temperature,[19] which affect the balance between Hund's rule coupling and crystal field effects. Also, in the current system, on hydration of $Na_{0.3}CoO_2$ to superconducting $Na_{0.3}CoO_2\cdot 1.3H_2O$, the layer thickness decreases significantly[14] though the electron count has remained constant.

Our proposal for relationships between the structural and electronic properties of Na_xCoO_2 is summarized in Fig. 6. The main panel shows the electronic phase diagram as we currently understand it.[6] The upper area shows a schematic representation of the Na distribution in the hexagonal layers, and the lower panel shows the ratio of the observed thickness of the CoO_2 layers in Na_xCoO_2 to that expected for layers of ideal octahedra. The "ideal" octahedral layer is derived by taking the lengths of the in-plane edges of the CoO_6 octahedra from the measured a lattice parameters and employing those values to calculate an ideal layer thickness, assuming 90° O—Co—O bond angles and equal Co—O bonds. We note that the CoO_2 layer is strongly compressed along the c axis to about of 85% of the expected thickness for ideal octahedra.

The smooth variation of CoO_2 layer thickness with x in the $H1$ phase suggests that in this part of the phase diagram the effect of changing Na content on the electronic properties of Na_xCoO_2, which changes from superconductor host metal, through charge ordered insulator, to antiferromagnetic metal, must be a consequence of the continuously changing electron count in the CoO_2 plane, and not a consequence of discontinuous changes in the types of electronic states that are mixed in at the Fermi energy. Continuous changes in the relative proportions of different types of states at E_F may be present, however, and mixing of the nominally empty e_g states with the t_{2g} and oxygen $2p$ states may be possible.[20]

In contrast, the $H2$ phase occurs in a composition region ($\sim 0.75<x<\sim 0.80$) of dramatic structural and electronic changes in Na_xCoO_2. Most significant from a structural viewpoint are the changes from occupancy of the off-center Na(2)′ sites in the $H1$ phase to the ideally triangular prismatic Na(2) sites in the $H2$ phase, and the rapid depopulation of the Na(1) sites. A discontinuous change in the CoO_2—CoO_2 layer separation is observed. This is accompanied by a substantial change in the electronic state of the CoO_2 layer, which rapidly increases in thickness in the $H2$ phase with increasing Na content. Whether these transitions

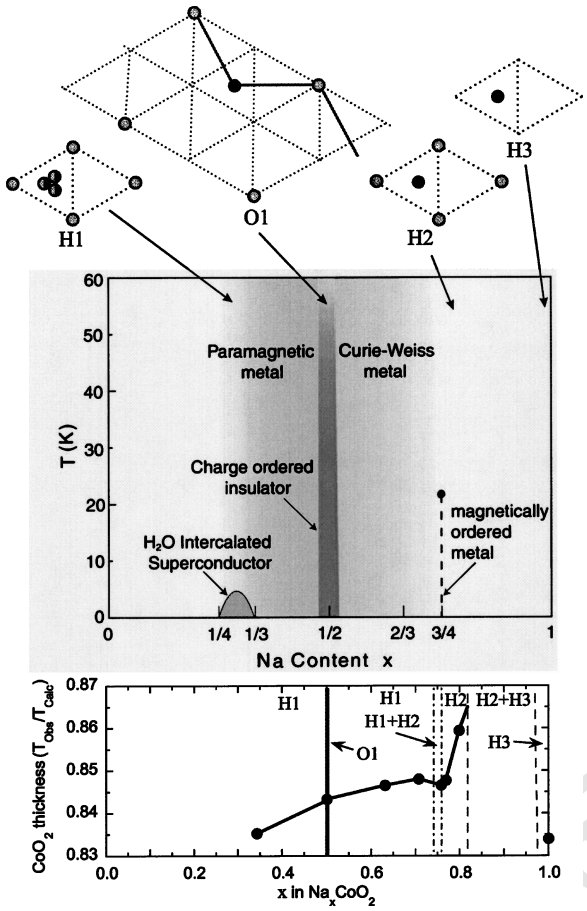

FIG. 6. Correspondence between structure and properties in Na_xCoO_2. Upper figure: schematic of the Na ion distributions in the four Na_xCoO_2 phases. Main panel: the electronic phase diagram. Lower panel: variation of the ratio of the observed CoO_2 layer thickness to the thickness of an ideal layer of octahedra.

are a response to the depopulation of the Na(1) sites, or are driven primarily by the change in electron count is not known, but a difference in the relative proportions of different electronic states at E_F must accompany them. Nothing is currently known about the physical properties of materials that have been clearly identified as being in the $H2$ phase. The abrupt changes in structure on passing from the $H1$ to the $H2$ structure are surprising, and the fundamentally different nature of these two phases is further supported by the two-phase region that separates them at ambient temperature. Further experimental and theoretical study of this transition may be of interest.

There is an abrupt decrease in the CoO_2 layer thickness on passing into the $H3$ phase, where the Na(2) sites are fully occupied in a long range ordered hexagonal lattice. $NaCoO_2$ is expected in the simplest picture ($3d^6Co^{3+}$) to be a band insulator with fully occupied t_{2g} orbitals. The decrease of the layer thickness on passing from the $H2$ to the $H3$ phase may reflect a change in the relative energies of filled t_{2g} states compared to other states near E_F at the d^6 electron count. The physical properties of the $H3$ $NaCoO_2$ phase are not currently known.

The insulating state at $Na_{0.5}CoO_2$ is found in a phase (the $O1$ phase) with a long-range ordered arrangement of zigzag Na chains, with Na atoms in both Na(1) and Na(2) sites, and an accompanying charge-ordered Co array. Metallic conductivity is observed in compounds with the $H1$ phase structure for x values surrounding $x=0.5$. The displaced Na(2)′ positions and the Na(1) occupancy in the average structure of the $H1$ phase, and the electron diffraction characterization, revealing rich variations of Na ordering schemes related to that found in $Na_{0.5}CoO_2$,[16] suggest that the Na ion array forms zigzag fragments, either disordered or in short-range ordered arrays, in the whole $H1$ composition region. These zigzag fragments appear to vary in number and distribution as the Na plane filling changes.[16] Even in preparations or at compositions where the Na ion distribution appears to be disordered, it is likely that such fragments appear on the short-range scale, much as disordered CuO_2 chain fragments are found in $YBa_2Cu_3O_{7-x}$.[21] Due to the low proportion of Na(1) occupancy in the $H2$ and $H3$ phases, such zigzag Na fragments are not expected to occur.

In conclusion, the structural characterization of Na_xCoO_2 by neutron and electron diffraction has resulted in a picture of how the sodium ions are arranged in the charge reservoir layer, and how the CoO_2 layers respond structurally to changes in electron count and Na ion distribution. These changes are similar in character to those seen in the high T_c superconductors, where structural and electronic degrees of freedom within a square conducting plane are often linked in a subtle manner (e.g., Ref. 22), suggesting that a similarly rich phenomenology remains to be fully elucidated in layered triangular conductors.

ACKNOWLEDGMENTS

This work was supported by NSF Grant No. DMR 0244254, by DOE BES Grant No. DE-FG02-98-ER45706, and also NSF Grant No. CHE-0314873.

[1] A.P. Ramirez, Annu. Rev. Mater. Sci. **24**, 453 (1994).
[2] R.J. Cava, Science **247**, 656 (1990).
[3] I. Terasaki, Y. Sasago, and K. Uchinokura, Phys. Rev. B **56**, R12 685 (1997).
[4] Yayu Wang, N.S. Rogado, R.J. Cava, and N.P. Ong, Nature (London) **423**, 425 (2003).
[5] K. Takada, H. Sakurai, E. Takayama-Muromachi, F. Izumi, R.A. Dilanian, and T. Sasaki, Nature (London) **422**, 53 (2003).
[6] Maw Lin Foo, Yayu Wang, Satoshi Watauchi, H.W. Zandbergen, Tao He, R.J. Cava, and N.P. Ong, cond-mat/0312174 (unpublished).
[7] Jun Sugiyama, Hiroshi Itahara, Jess H. Brewer, Eduardo J. An-

saldo, Teruki Motohashi, Maarit Karppinen, and Hisao Yamauchi Phys. Rev. B **67**, 214420 (2003).
[8] T. Motohashi, R. Ueda, E. Naujalis, T. Tojo, I. Terasaki, T. Atake, M. Karppinen, and H. Yamauchi, Phys. Rev. B **67**, 064406 (2003).
[9] S. Bayrakci, C. Bernhard, D. P. Chen, B. Keimer, R. K. Kremer, P. Lemmens, C. T. Lin, C. Niedermayer, and J. Strempfer, Phys. Rev. B **69**, 100410 (2004).
[10] C. Delmas, J.J. Braconnier, C. Fouassier, and P. Hagenmuller, Solid State Ionics **3–4**, 165 (1981).
[11] C. Fouassier, G. Matejka, J.-M. Reau, and P. Hagenmuller, J. Solid State Chem. **6**, 532 (1973).
[12] Y. Ono, R. Ishikawa, Y. Miyazaki, Y. Ishii, Y. Morii, and T. Kajitani, J. Solid State Chem. **66**, 177 (2002).
[13] R.J. Balsys and R.L. Davis, Solid State Ionics **93**, 279 (1996).
[14] J.W. Lynn, Q. Huang, C.M. Brown, V.L. Miller, M.L. Foo, R.E. Schaak, C.Y. Jones, E.A. Mackey, and R.J. Cava, Phys. Rev. B **68**, 214516 (2003).
[15] J.D. Jorgensen, M. Avdeev, D.G. Hinks, J.C. Burley, and S. Short, Phys. Rev. B **68**, 214517 (2003).
[16] H.W. Zandbergen, M.L. Foo, Q. Xu, V. Kumar, and R.J. Cava, cond-mat/0403206 (unpublished).
[17] A. Larson and R.B. Von Dreele, Los Alamos National Laboratory internal report (1994).
[18] Q. Huang, M.L. Foo, J.W. Lynn, H.W. Zandbergen, G. Lawes, Yayu Wang, B. Toby, A.P. Ramirez, N.P. Ong, and R.J. Cava, cond-mat/0402255 (unpublished).
[19] I.A. Nekrasov, S.V. Streltsov, M.A. Korotin, and V.I. Anisimov, Phys. Rev. B **68**, 235113 (2003).
[20] C.A. Marianetti, G. Kotliar, and G. Ceder, cond-mat/0312514 (unpublished).
[21] J. D. Jorgensen, S. Pei, P. Lightfoot, H. Shi, A. P. Paulikas and B. W. Veal, Physica C **167**, 571 (1990).
[22] J. D. Jorgensen, in *Advances in Superconductivity XII*, edited by T. Yamashita and K. Tanabe (Springer-Verlag, Tokyo, 2000), pp. 9–14.